Terr. Atmos. Ocean. Sci., Vol. 21, No. 5, 807-816, October 2010 doi: 10.3319/TAO.2010.01.03.01(TT)

Seismic Velocity Structure and Improved Seismic Image of the Southern Depression of the Tainan Basin from Pre-Stack Depth Migration

Qunshu Tang[1, *] and Chan Zheng[2]

[1] *Key Laboratory of Marginal Sea Geology, South China Sea Institute of Oceanology, Chinese Academy of Sciences, Guangzhou 510301, China*
[2] *College of Informatics, South China Agricultural University, Guangzhou 510642, China*

Received 1 July 2009, accepted 3 January 2010

ABSTRACT

In this paper, a velocity model of the Southern Depression of the Tainan Basin is obtained along with its migrated image from an iterative pre-stack depth migration approach. The Cenozoic strata are uniformly layered with velocities varying from ~1.8 to ~3.6 km s^{-1}. However, the general velocity is slightly lower in the NW segment than the SE. Both fractures and burial depth might be the controls of their seismic velocities. There is an unconformable contact between the Cenozoic and underlying Mesozoic strata with an abrupt velocity jump from ~3.2 to ~4.3 km s^{-1}. The Mesozoic strata are recognized with acoustically distinct reflection patterns (chaotic, deformed and discontinuous) and complex internal structures (uplift, folds and faults). Their interval velocities range from ~4.3 to ~4.7 km s^{-1} within a depth from ~3.5 down to ~12.5 km, and the maximum depositional thickness reaches up to 6.5 km. Multiple tectonic events such as collision, subsidence and uplift might be responsible for the complexity of the Mesozoic strata.

Key words: Northern South China Sea, Tainan Basin, Velocity structure, Residual moveout velocity analysis, Pre-stack depth migration

Citation: Tang, Q. and C. Zheng, 2010: Seismic velocity structure and improved seismic image of the Southern Depression of the Tainan Basin from pre-stack depth migration. Terr. Atmos. Ocean. Sci., 21, 807-816, doi: 10.3319/TAO.2010.01.03.01(TT)

1. INTRODUCTION

The Tainan Basin (or Taixi'nan Basin, TNB in brief), located offshore southwestern Taiwan, is one of the typical Cenozoic polyhistory basins along the northeastern margin of South China Sea (Fig. 1). It extends from coastal plain, continental shelf, continental slope, to abyssal region with three NE-striking blocks: the Northern Depression, the Central Uplift Zone and the Southern Depression (Yu and Lin 1991; Lin et al. 2003; Ding et al. 2008). Many researchers are intrigued by the perplexing basin structures and evolution history as well as the resource potential. Numerous results from gravity, magnetic, geothermal, seismic, and well-logs were reported to provide us a comprehensive knowledge of the basin evolution (e.g., Sibuet et al. 2002; Lin et al. 2003; Hsu et al. 2004; Chen 2006; Wang et al. 2006; Li et al. 2007; Shi et al. 2008). As an important physical parameter, the seismic velocity can provide more derived information to constrain the substructures, such as density, porosity, lithology and chronology. Unfortunately, besides the scarcely deployed OBS (Ocean Bottom Seismometer) observations (e.g., Wang et al. 2006) and the rarely published well logs (e.g., Chen 2006), the velocity structures of the TNB are still poorly understood, especially in the Southern Depression where there is no drilling thus far.

Although the conventional seismic images are widely used to constrain the morphological features of the substructures, the imaging-dependent stacking velocities are rarely used (Yu and Lin 1991). These are not only because the time-domain stacking velocity is short of direct geological meanings, but also the conventional Dix interval velocity (Dix 1955) has fatal shortcomings, such as severe instability and lateral distortions (Tillard and Dubois 1995). However, an accurate velocity model is critical for improving seismic images. Fortunately, the pre-stack depth migration, which has the ability of self-checking, provides a powerful velocity analysis scheme. In this paper, we use an iterative velocity

* *Corresponding author*
E-mail: tqsh@scsio.ac.cn

analysis approach based on residual moveout (RMO) and velocity perturbation theory developed by Liu (1995) to obtain the velocity structures. Hereafter, we call this approach a "residual moveout velocity analysis" (RMOVA in brief).

In order to obtain a more "geologically reasonable" velocity model, the objective interface (reflector) is determined by a combined scheme of both data-driven and structure-dependent (Kim et al. 1996; Alaei 2006). Any a priori knowledge that constrains the solution without hindering it is welcome (Versteeg 1993). For the case of the South Depression of the TNB, the only a priori information comes from seismic interpretation of the time sections, e.g.,

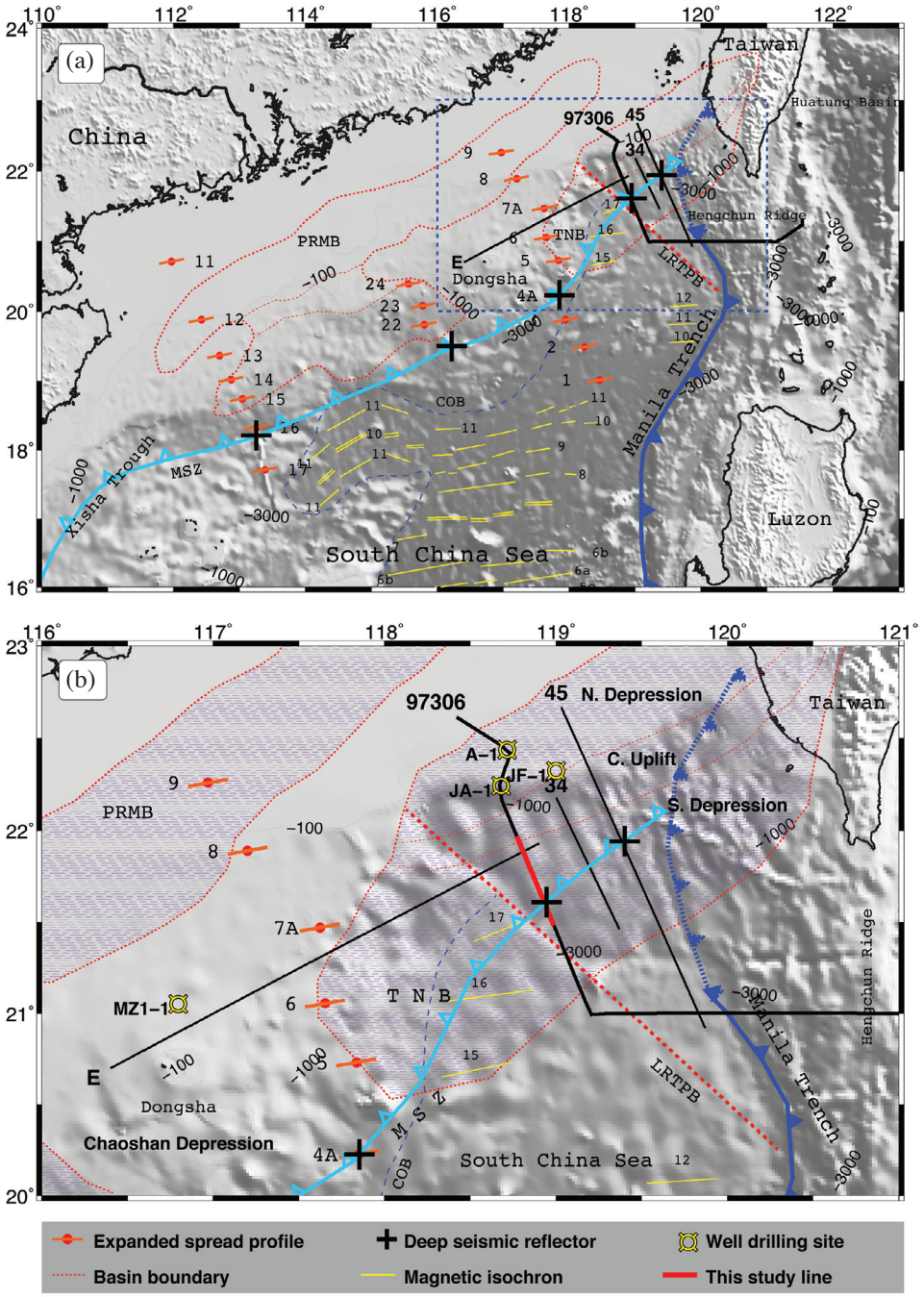

Fig. 1. (a) Map of the survey lines and regional tectonic divisions overlaid on the topography image (data from http://topex.ucsd.edu) of the northeastern South China Sea. Seismic lines (black lines) and expanded spread profiles (orange bars) are presented. The main tectonic units, boundaries and magnetic lineations are integrated from previous research (Briais et al. 1993; Hsu et al. 2004; Li et al. 2007), including MSZ: Mesozoic Suture Zone, COB: Continental Oceanic Boundary, LRTPB: Luzon-Ryuku Transform Boundary, PRMB: Pearl River Mouth Basin, and TNB: Tainan Basin. (b) Detailed map of the TNB as outlined with blue dashed box in (a). The red segment of Line 97306 is our interested profile in this study (shown in Figs. 2, 5 and 6). The well drilling sites around and the structural division of the TNB are presented.

reported by Sibuet et al. (2002) and Li et al. (2007). This will make the velocity analysis far more effective when it is strongly linked to the interpreted substructures (Fagin 1999). A final accurate velocity model as well as its pre-stack depth migrated image with high clarity are expected.

2. OVERVIEW OF THE STUDY REGION

From the Late-Triassic to Early-Cretaceous, the South China continental margin experienced extensive abyssal to neritic depositional phases (Zhou 2002; Lin et al. 2003; Shao et al. 2007; Hao et al. 2009). The change in the tectonic regime from an active to a passive margin starting from ~50 Ma led to the development of a series of Cenozoic rift basins and the opening of South China Sea (Taylor and Hayes 1980, 1983; Briais et al. 1993; Hall 1997, 2002; Li et al. 2007). The TNB is such a kind of basin that the Cenozoic sediments overlapped unconformably on the Mesozoic depositional system. Drilling data reveal the stratigraphic hiatus from the Upper-Cretaceous to Lower-Palaeocene and indicate a prolonged episode of uplifting and erosion during the period (about 110 - 60 Ma)(Lin et al. 2003; Xia et al. 2004; Li et al. 2008).

The TNB is filled with a succession of the Oligocene to Quaternary sediments. A series of regional stratigraphic sequences has been recognized based on the seismic and well data, and a set of the detailed stratigraphic models has been proposed (e.g., Huang et al. 2001; Lin et al. 2003; Yi et al. 2007; Ding et al. 2008). For instance, Lin et al. (2003) proposed that there were three stages of deposition during the Cenozoic, named syn-rift (~58 - 37 Ma), post-breakup (~30 - 6.5 Ma) and foreland basin (~6.5 - 0 Ma), respectively. On the contrary, the Mesozoic evolution beneath the TNB is seldom discussed due to few trustful stratigraphic evidences.

Most of the Southern Depression of the TNB is in a hemipelagic-abyssal environment today. Seismic reflections reveal that the Cenozoic sequences are quite parallel and continuous (Fig. 2; Li et al. 2007; Ding et al. 2008; Lin et al. 2008). Until now, there was no available drilling evidence taken from the Southern Depression. Therefore, wells A-1, JA-1, JF-1 (Chen 2006) in the Northern Depression of the TNB and well MZ1-1 in the ChaoShan Depression nearby (Li et al. 2008) are tied to the seismic profiles (Fig. 1). More importantly, previous seismic interpretations of the Southern Depression (Fig. 2; Yan et al. 2006; Li et al. 2007; Yi et al. 2007; Ding et al. 2008) have been hampered by the apparently variable character, unclear imaging, devoid of accurate velocity information and a geologically meaningful depth profile. We address these problems by using the iterative pre-stack depth migration to refine the velocity model and to generate an improved depth image.

3. DATA ACQUISITION AND PROCESSING

In 2001, a seismic survey labeled 97306 was carried out by the Guangzhou Marine Geological Survey of the Chinese Ministry of Land and Resources. It traversed perpendicularly to the strike of the three blocks of the TNB (Fig. 1). The source was composed of four arrays of Sleeve guns (total volume of 3000 cubic inch) and was triggered every 50 m at a depth of 7 m. The data were collected using

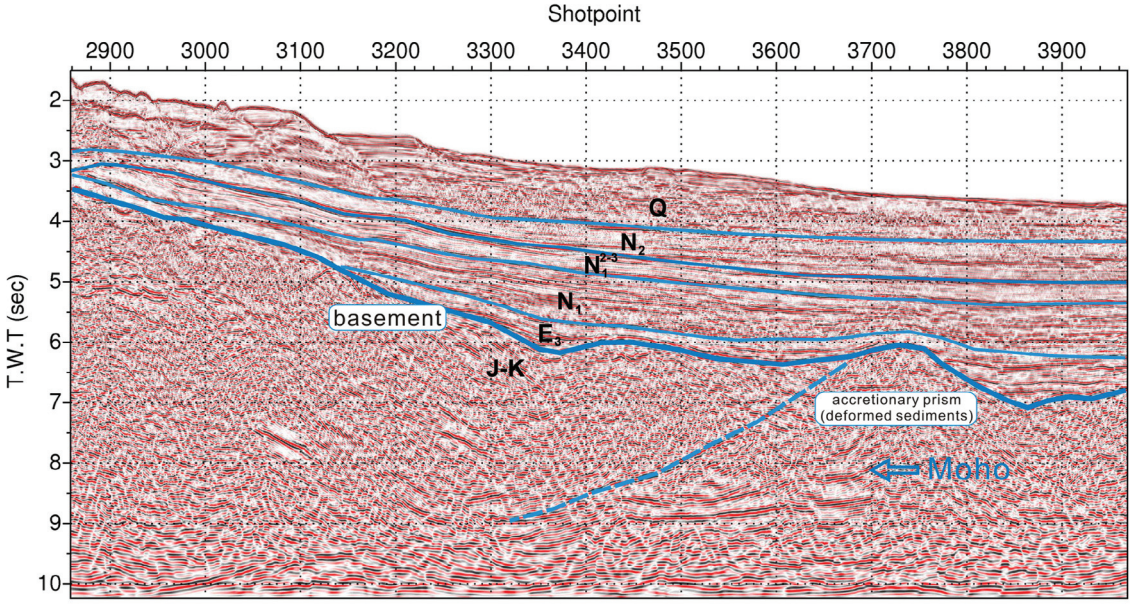

Fig. 2. Migrated time section of this study line (see location in Fig. 1) overlapped with the geological interpretations from Sibuet et al. (2002) and Li et al. (2007). TWT = two way travel time.

a 240-channel streamer with 12.5 m channel spacing towed at a depth of 9 m. The record length was 10.998 s with a sampling rate of 2 ms.

We chose the section with shot points ranging from 2861 (NW) to 4030 (SE) in the Southern Depression (thick red line in Fig. 1) for our study. In order to adapt to our computational capability, the data were reasonably re-sampled temporally and spatially under the restriction of Nyquist frequencies. The essential data parameters are as follows: sample rate 4 ms, record length 10.024 s, channels 120, shot interval 50 m, receiver interval 25 m, near offset 250 m, far offset 3225 m.

In the RMOVA approach, velocity analysis is based on the principle that the image in the migrated data will be distorted when an erroneous velocity is used, and the difference of the imaged depths (i.e., RMOs) at a common image gather (CIG) is a measure of the velocity error. Therefore, the quantitative relationship between RMO and residual velocity is used to update a new velocity iteratively. This approach has several outstanding advantages wherein, no limitation on offset, dip, and velocity distribution is present if the velocity perturbation is sufficiently small (Liu 1995; Liu and Bleistein 1995; Liu 1997). In practice, it is a layer-stripping method, in a top-down procedure to determine the velocity model. The efficient Kirchhoff migration is used at each iteration; the resultant CIGs are used to estimate the residual velocity.

However, it is very expensive to conduct RMOVA iterations especially for a large dataset. In order to reduce the iteration times and enhance the reliability of velocity estimation for the whole profile, a quantitative velocity analysis has been carried out for a smaller data set of shot-points 3461 to 3760 as the trial section. There are three essentials considered for a proper initial velocity: (1) the basic knowledge of the strata velocities, (2) the velocity trend of the next layer predicted from the CIGs, and (3) the convergent direction during the iterations. After multi-iterations of the RMOVA, the resultant velocities are used to limit the model space while giving the initial velocities for the whole profile; therefore, only one iteration was implemented.

First, a constant velocity (1500 m s^{-1}) model was used to migrate the data. Since a correct seawater velocity was used, the seafloor was correctly imaged. Second, after picking the seafloor interface, a two-layer velocity model with a fixed velocity 1500 m s^{-1} in the first layer and an initial velocity of 1800 m s^{-1} (derived from the trial section) in the second layer was constructed for migration. Third, the migrated data were sorted into CIGs, and some of them were chosen for depth measuring, RMO and velocity updating. Then, a velocity of 1803 m s^{-1} was settled as the interval velocity of the second layer. Following the iterative procedure, a final velocity model with all interested layers was constructed.

Things are different for the deeper layers. Several factors degraded the quality of seismic imaging, such as lower signal-to-noise ratio, weaker reflected energy, discontinuous reflectors, etc. To overcome the lower sensitivity of the RMOVA in the deep layers, an optimal migrated image and its focused RMO semblances (Fig. 3) for specific GIGs are used as the additional criteria of velocity determination. By sweeping the velocities in the repeated migration, we found that a velocity perturbation of 100 m s^{-1} could produce an obvious image quality variation. Finally, an average velocity range was fixed and one preferred velocity was fixed as the final result.

4. RESULTS

The RMOVA scheme has been applied successfully to determine the velocity structures of the Southern Depression of the TNB. In this section, the results from pre-stack migration (e.g., flattened CIGs, focused CIG semblances) are shown as solid evidence of the estimated velocity model. Meanwhile, an enhanced image with a maximum depth around 15 km is presented.

Figure 3 shows an example of RMOVA. Figure 3a shows a CIG at 35000 m (CIG-35000) relative to the first shot point. The flatness of the events indicates the goodness of the final velocity model. A semblance analysis of CIG-35000 is presented in Fig. 3b. Here, semblance peaks of the events all focus near the zero r-parameter line ($r = [z(h)^2 - z_0^2] / h^2$, where z is the depth at the offset h, z_0 is the depth at zero offset), indicating that the velocity model (Fig. 3c) is nearly correct. Conversely, the noise such as multiples cannot be flattened or correctly focused (Figs. 3a, b).

The semblance analysis for 19 CIGs (each 3 km apart) along the whole profile is presented in Fig. 4. Note that the semblance peaks are centered along the zero r-parameter line vertically, and correlated with the picked interfaces laterally. From these results, the following conclusion can be drawn: because of the moderate complexity of the study region, a constant or linear velocity versus distance/depth is sufficient to represent the velocity of the layer.

Figure 5 is the contoured map of the final interval velocity model obtained from the RMOVA. Generally, the upper layers have a higher resolution than the lower layers. The velocity variation from ~1800 to ~3600 m s^{-1} is a typical range of Cenozoic strata (Layers 2 - 5, e.g., Li et al. 2007). As aforementioned, there are little or weak constraints on the deeper layers to ensure a good resolution. Taking layer 7 as an example, the discontinuous deep reflectors at ~11 and ~35 km are the only constraints from the data. Additionally, the seismic interpretation of pre-Jurassic [from tieline E (Fig. 1), Li et al. 2008] depositional sequences (Figs. 2, 6) were used as the reference of velocity range. So, a probably reasonable velocity of 4.7 km s^{-1} was set for layer 7. A velocity of 5.5 km s^{-1} was given for layer 8 as the general crystalline crust without any other constraints.

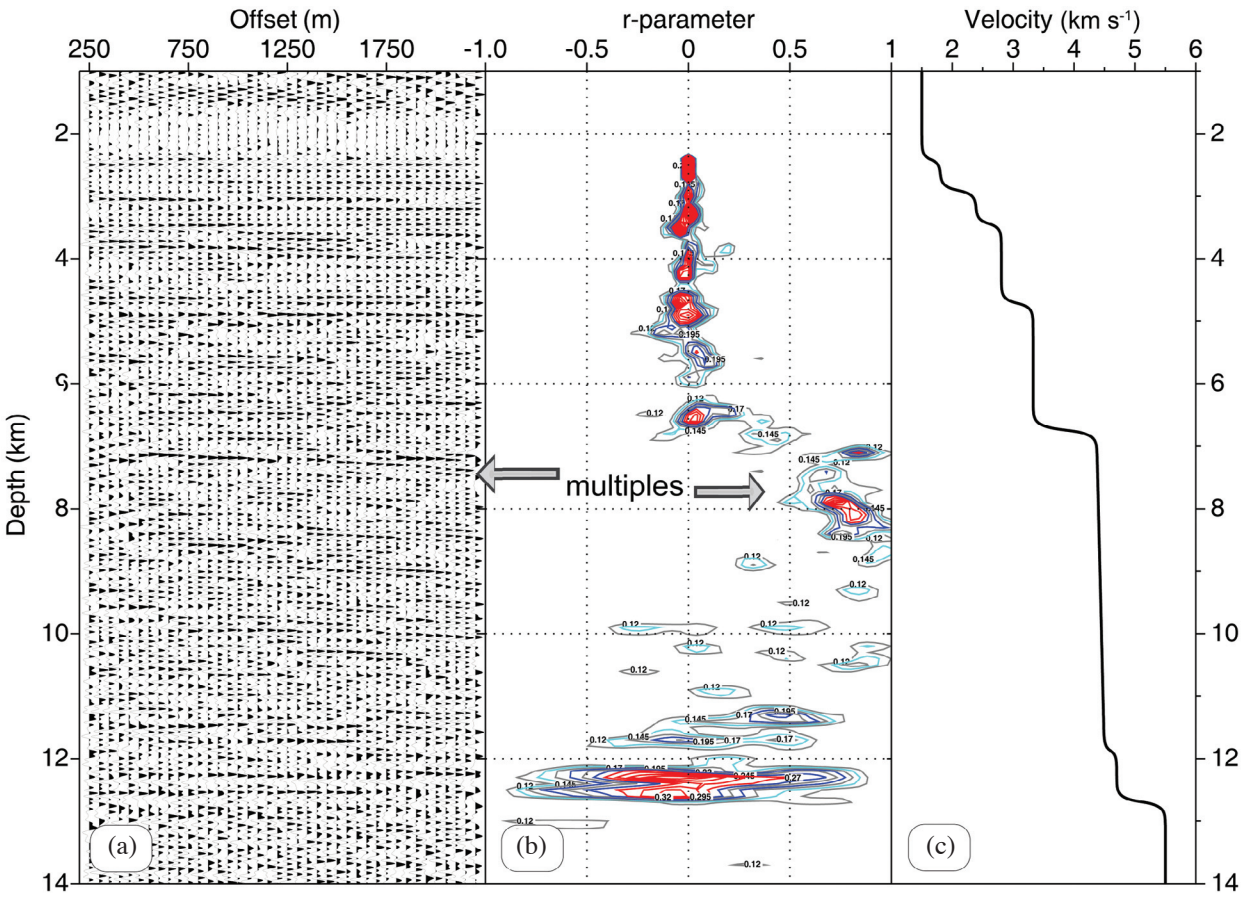

Fig. 3. Residual moveout velocity analysis of the CIG at 35000 m. (a) CIG after pre-stack depth migration. (b) Semblance contour map of the selected CIG in (a). The r-parameter represents the velocity error. (c) The corresponding interval velocity model at CIG-35000.

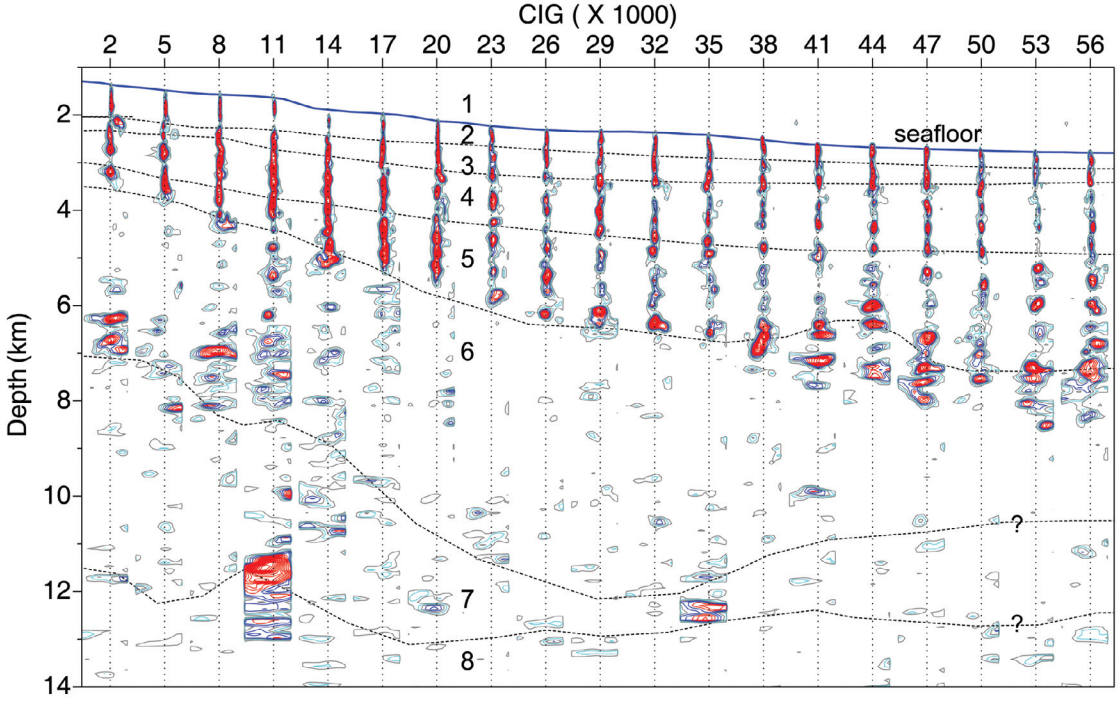

Fig. 4. Semblance analysis (same as Fig. 3b) for 19 CIGs along the whole profile, each 3 km apart. The picked velocity boundaries are denoted with blue (seafloor) and gray (subsurfaces) lines. Velocity layers are numbered top-down.

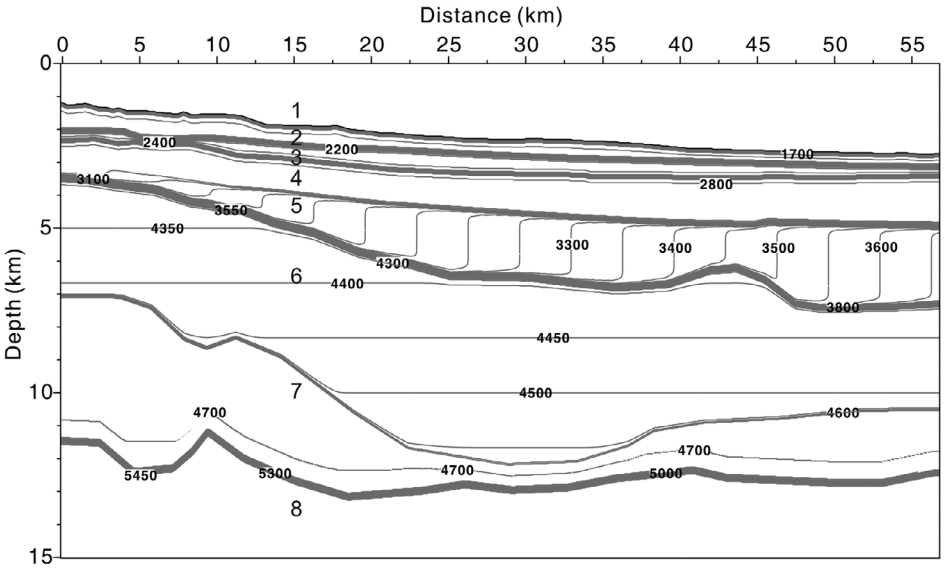

Fig. 5. The contour map of the final interval velocity model estimated from RMOVA.

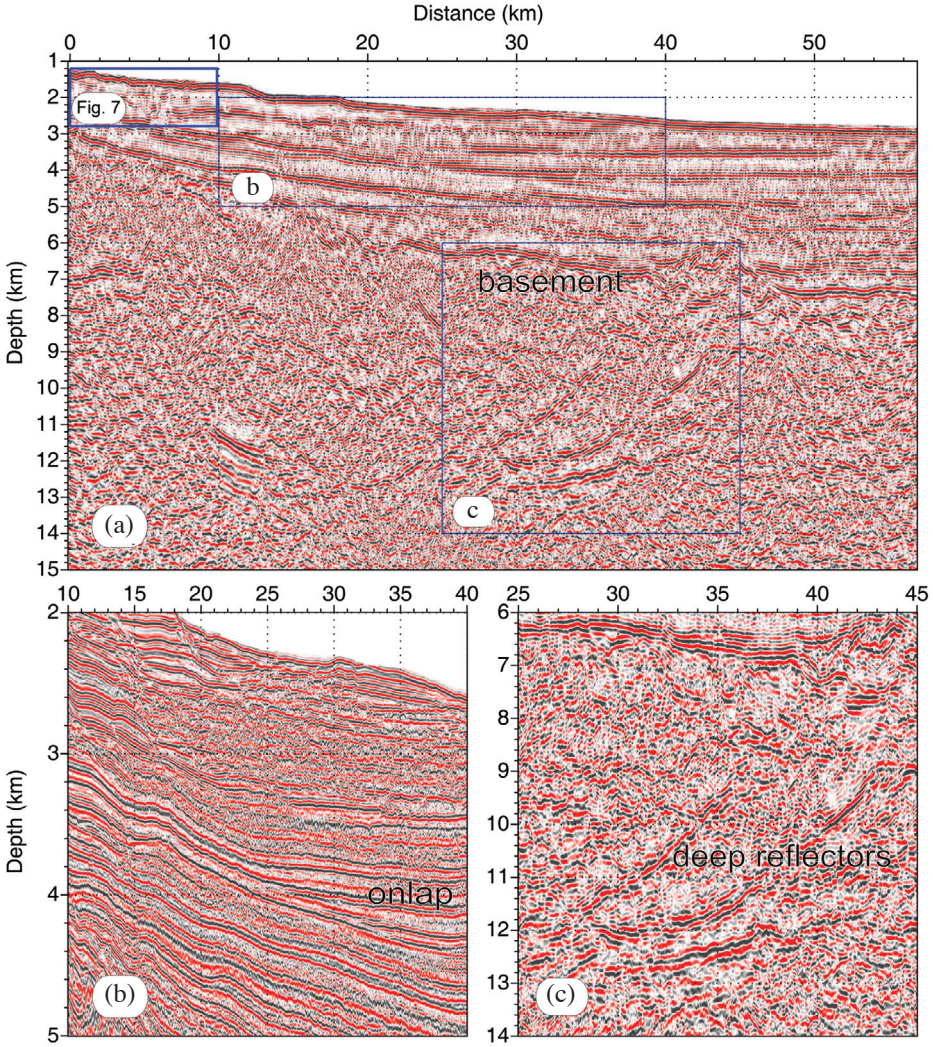

Fig. 6. (a) The final pre-stack depth migrated image (stacked in offset domain, AGC and filtering applied) with the estimated velocity model in Fig. 5. (b), (c) show the Cenozoic and the Mesozoic erathem, respectively [see their locations in (a)].

The interval velocity model reinforces and increases our knowledge of this region. First, the general velocity variation is in accordance with the chronostratigraphic framework (Li et al. 2007; Yi et al. 2007; Ding et al. 2008). Second, the burial depth might be an important factor influencing layer velocity. Layer velocities are obviously higher beneath the deeper water area where the burial depth becomes deeper laterally (e.g., layers 5, 6). Third, an abrupt velocity jump from ~3.2 to ~4.3 km s^{-1} between layer 5 and layer 6 leads us to believe that it is not only a strong acoustic boundary, but also a distinct unconformity between the Cenozoic and Mesozoic strata. This unconformity has been encountered by several drillings (e.g., Chen 2006). Fourth, the meta- or deformed sediments of the Mesozoic strata (layers 6, 7; Sibuet et al. 2002; Ding et al. 2008) reach down to ~12.5 km depth with a maximum depositional thickness of ~6.5 km, indicating that they are apt to be altered by later tectonic subsidence or accretion.

With the velocity model, the depth-migrated image is obtained as shown in Fig. 6 and has been significantly improved compared with the time image (Fig. 2). The Cenozoic sediments are shown with clear acoustic interfaces as well as detailed internal horizons and stratigraphic relationships (Figs. 6b, 7). The chaotic, deformed and discontinuous reflection patterns are distinct features of the Mesozoic strata. Nonetheless, the main seismic horizons and internal structures can be seen easily. The tectonically induced structures (faults, uplift, folds, etc.) are also clearly imaged (Figs. 6a, c). These phenomena strongly suggest that this region has experienced complex tectonic events which are still under debate (Yao et al. 1994; Hayes et al. 1995; Hsu et al. 2004; Li et al. 2007).

5. DISCUSSION

In the study, we investigated the velocity structure of the Southern Depression of the TNB using the iterative pre-stack depth migration scheme. Meanwhile, a clearly migrated image is presented to justify the estimated velocity model and to reveal the detailed internal structures. Here, some facts should be reaffirmed prior to the interpretation of the velocity structure and its migrated image. (I) Velocity resolution is the most pertinent issue. Synthetic modeling shows that the resultant velocity is quite close to the true value (e.g., Liu 1997). (II) The velocity layering is both geologically and acoustically dependent, but not fitting exactly with the geological interpretation of the time section. (III) A constant or linear velocity is sufficient to represent the interval velocity because of the moderate complexity of this region. (IV) Velocities of the deeper layers are less constrained. (V) A careful interpretation of the migrated section will be presented mainly focusing on the Mesozoic strata.

Previous reports on velocity structures in the TNB are rare, especially in the Southern Depression. So far, seismic velocities are seldom analyzed for deciphering the seismic record in this region. The linkage between seismic lines and the drillings nearby (Chen 2006) provides us useful but limited information to support our results.

On the whole, velocities of the Cenozoic strata (layers 2 - 5, from the Oligocene to present) are uniformly layered.

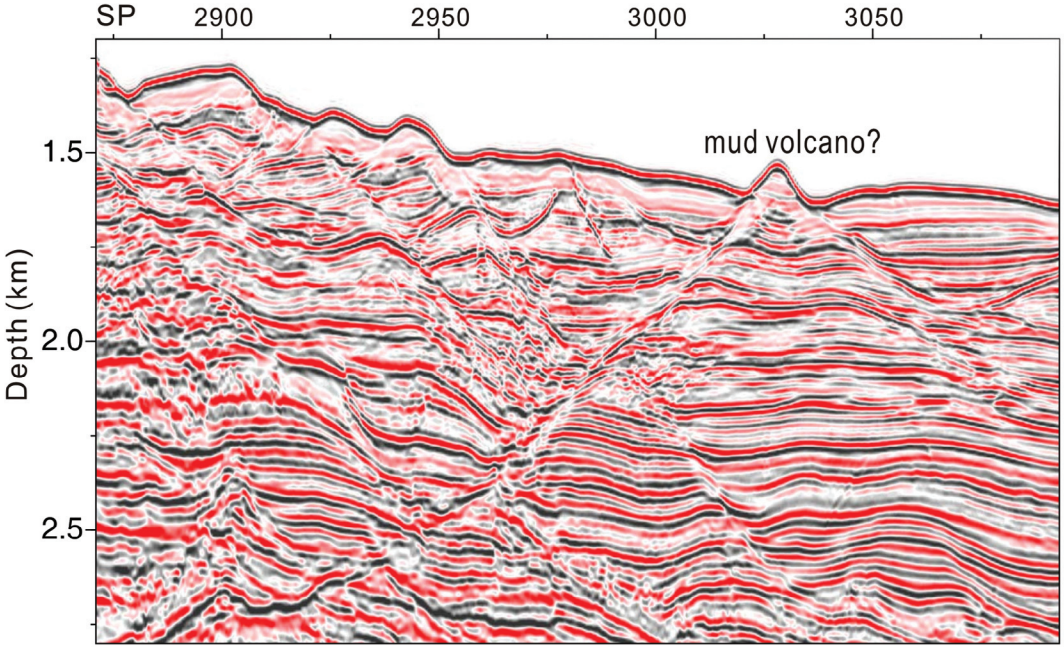

Fig. 7. The NW segment of the improved profile shows a complex substructure caused by dense fractures. SP = shot point. See Fig. 6a for location.

A slow-rifting tectonic setting and a deep-water dominated depositional environment might be responsible for the structures of the Southern Depression (Zhou et al. 2005; Li et al. 2007; Ding et al. 2008). The situation is slightly different in the NW segment near the Central Uplift: the slope failure caused by gravity instability (Yan et al. 2006) makes the substructures more complex. The dense fractures developed with a shallower burial depth of the strata make the velocity slightly lower than the SE segment (Figs. 5, 7, 8), agreeing well with a previous study (Chen and Yang 1996). Moreover, the enhanced depth image reveals that there should not be a mud volcano (Fig. 7; Yan et al. 2006) at the slope, but a fault-induced relict stratum with both sides slumped as outlined in Fig. 8. This is since there are the parallel reflectors beneath the dome-like structure, instead of the columnar acoustic blanking caused by fluid upward migration (Chiu et al. 2006).

Drillings reveal that the encountered Mesozoic strata are the Upper Jurassic to Lower Cretaceous sedimentary rocks and velocities vary from 3.6 to 5.0 km s^{-1} (Chen and Yang 1996; Lin et al. 2003; Chen 2006; Li et al. 2007; Shao et al. 2007). Seismic refraction observation in the Chaoshan Depression neighboring the TNB reported that the velocities of the top Mesozoic strata are around 4.0 ± 0.5 km s^{-1} (Lü et al. 2009). So we believe that our measured velocity values (4.3 - 4.7 km s^{-1}) of layer 6 and layer 7, which fall in the velocity range of typical sedimentary or meta-sedimentary rocks, are reasonable. Meanwhile, the deformed internal acoustic features within the layers are identified as the sedimentary layers (Figs. 6, 8). These features are also seen in other experiments (e.g., Sibuet et al. 2002). The determination of the sedimentary strata is important to our suggestion that the thick sediments with great burial depth in the Southern Depression were caused by complex tectonic evolutions. The Cretaceous collision and the change of the tectonic regime of the region from active to passive from the Late Oligocene (e.g., Taylor and Hayes 1980; 1983; Li et al. 2007) might be responsible for the accretion and the subsidence of the Mesozoic strata along the weak trough-like suture zone, respectively. Furthermore, the clearly imaged internal deep faults, folds and accretionary prism (Figs. 6, 8), which developed only in the Mesozoic strata, might be the evidence of a compressional regime during the collision period. Therefore, rifting, subduction, or collision could be the candidates of the local dynamic controls.

According to the velocity model (Fig. 5) and the imaged deep reflectors (Figs. 6a, c), we think that the interpretation of the "Moho discontinuity" at a depth of ~11 km (8.3 sec in time section, Fig. 2; Li et al. 2007; Ding et al. 2008) should be reconsidered. An unreasonably sharp velocity contrast would be expected if the reflector was interpreted as Moho, since our measured velocity is only about 4.7 km s^{-1} just above the "Moho." Based on the assumption of a suture zone from numerous previous studies (e.g., Liu et al. 2006), we prefer the strong deep reflectors ("Moho") to be fault surfaces relating to the underthrusting. We agree with the possible explanation for this strong reflectivity that the presence of mylonites within the fault zone may produce the strong reflections (Hayes et al. 1995).

6. CONCLUSION

Velocity structures can provide insights into the nature of the Earth's substructures. In this paper, a velocity model of the Southern Depression of the TNB is presented along with the enhanced image from an iterative pre-stack depth

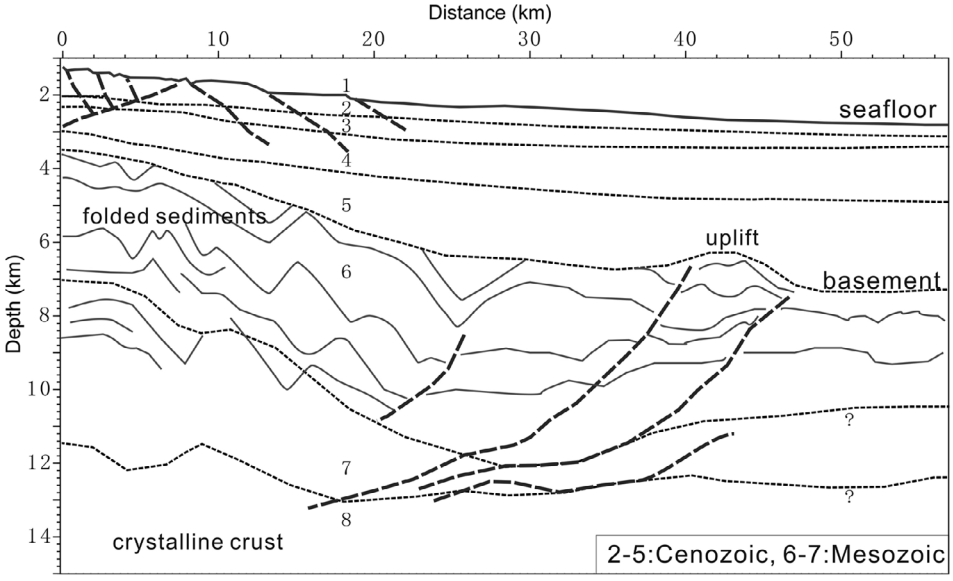

Fig. 8. Interpretations of the pre-stack depth migrated image in Fig. 6a. More detailed structures of the Mesozoic erathem are presented.

migration approach. The Cenozoic strata are uniformly layered with velocities varying from ~1.8 to ~3.6 km s^{-1}. However, the general velocity is slightly lower in the NW segment than the SE. Both fractures and burial depth might be the control factors of their seismic velocities. Looking either from the acoustic features and the migrated image, an unconformity can be traced easily between the Mesozoic and the overlying Cenozoic strata with an abrupt velocity drop from ~4.3 to ~3.2 km s^{-1}. The Mesozoic strata are recognized with acoustically distinct reflection patterns (chaotic, deformed and discontinuous) and complex internal structures (uplift, folds and faults). The interval velocities range from ~4.3 to ~4.7 km s^{-1} within a depth from ~3.5 down to ~12.5 km, and the maximum depositional thickness reaches up to 6.5 km. Multiple tectonic events such as collision, subsidence, and uplift might be responsible for the complexity of the Mesozoic strata. Moreover, our results support the contention that the strong deep reflectors might be fault surfaces along the suture zone, rather than the "Moho discontinuity" alluded to from previous interpretations.

Acknowledgements We thank the R/V Tanbao crew for the data acquisition. We appreciate the beneficial discussions with Prof. Pin Yan, Prof. Xiaobin Shi, Dr. Hailing Liu, and Senior Engineer Hujun Hao. Reviewers are greatly thanked for their thorough work and many helpful comments. Seismic Unix (Cohen and Stockwell 2008) was used to accomplish our data analysis. Generic Mapping Tools (GMT; Wessel and Smith 1998) was used for preparing Fig. 1. This research is supported financially by the Knowledge Innovation Program of the Chinese Academy of Sciences (Grants kzcx2-yw-228 and SQ200908), the National Natural Science Foundation of China (Grants 40904011, 40876027, and U0733003), the National Basic Research Program of China (Grant 2007CB411706), and the Open Fund of CAS Key Laboratory of Marginal Sea Geology, South China Sea Institute of Oceanology (Grant MSGL08-18).

REFERENCES

Alaei, B., 2006: An integrated procedure for migration velocity analysis in complex structures of thrust belts. *J. Appl. Geophys.*, **59**, 89-105, doi: 10.1016/j.jappgeo.2005.08.004. [Link]

Briais, A., P. Patriat, and P. Tapponnier, 1993: Updated interpretation of magnetic anomalies and seafloor spreading stages in the South China Sea: Implications for the tertiary tectonics of southeast Asia. *J. Geophys. Res.*, **98**, 6299-6328, doi: 10.1029/92JB02280. [Link]

Chen, A. T. and Y. L. Yang, 1996: Lack of compressional overprint on the extensional structure in offshore Tainan and the tectonic implications. *Terr. Atmos. Ocean. Sci.*, **7**, 505-522.

Chen, M. L., 2006: Sediment velocity structures in the Taiwan Strait and the coastal plain of west Taiwan. Master Thesis, Institute of Geophysics, National Central University, Jhongli, Taiwan, ROC, 110 pp.

Chiu, J. K., W. H. Tseng, and C. S. Liu, 2006: Distribution of gassy sediments and mud volcanoes offshore southwestern Taiwan. *Terr. Atmos. Ocean. Sci.*, **17**, 703-722.

Cohen, J. K. and J. J. W. Stockwell, 2008: CWP/SU: Seismic Un*x Release No. 41, an open source software package for seismic research and processing, Center for Wave Phenomena, Colorado School of Mines, Golden, USA.

Ding, W. W., J. B. Li, M. B. Li, X. L. Qiu, Y. X. Fang, and Y. Tang, 2008: A Cenozoic tectono-sedimentary model of the Tainan Basin, the South China Sea: Evidence from a multi-channel seismic profile. *J. Zhejiang Univ. Sci. A*, **9**, 702-713, doi: 10.1631/jzus.A071572. [Link]

Dix, C. H., 1955: Seismic velocities from surface measurements. *Geophysics*, **20**, 68-86, doi: 10.1190/1.1438126. [Link]

Fagin, S., 1999: Model based depth imaging. SEG Course Notes, series 10.

Hall, R., 1997: Cenozoic plate tectonic reconstructions of SE Asia. In: Fraser, A. J., S. J. Matthews, and R. W. Murphy (Eds.), Petroleum Geology of Southeast Asia, Geological Society, London, Special Publications, 126, 11-23, doi: 10.1144/GSL.SP.1997.126.01.03. [Link]

Hall, R., 2002: Cenozoic geological and plate tectonic evolution of SE Asia and the SW Pacific: Computer-based reconstructions, model and animations. *J. Asian Earth Sci.*, **20**, 353-431, doi: 10.1016/S1367-9120(01)00069-4. [Link]

Hao, H., X. Zhang, H. You, and R. Wang, 2009: Characteristics and hydrocarbon potential of Mesozoic strata in eastern Pearl River Mouth basin, northern South China Sea. *J. Earth Sci.*, **20**, 117-123, doi: 10.1007/s12583-009-0013-4. [Link]

Hayes, D. E., S. S. Nissen, P. Buhl, J. Diebold, B. Yao, W. Zeng, and Y. Chen, 1995: Throughgoing crustal faults along the northern margin of the South China Sea and their role in crustal extension. *J. Geophys. Res.*, **100**, 22435-22446.

Hsu, S. K., Y. C. Yeh, W. B. Doo, and C. H. Tsai, 2004: New bathymetry and magnetic lineations identifications in the northernmost South China Sea and their tectonic implications. *Mar. Geophys. Res.*, **25**, 29-44, doi: 10.1007/s11001-005-0731-7. [Link]

Huang, C. Y., K. Xia, P. B. Yuan, and P. G. Chen, 2001: Structural evolution from Paleogene extension to Latest Miocene-Recent arc-continent collision offshore Taiwan: Comparison with on land geology. *J. Asian Earth Sci.*, **19**, 619-639, doi: 10.1016/S1367-9120(00)00065-1. [Link]

Kim, Y. C., C. M. Samuelsen, and T. A. Hauge, 1996: Effi-

cient velocity model building for prestack depth migration. *The Leading Edge*, **15**, 751-753.

Li, C. F., Z. Zhou, J. Li, H. Hao, and J. Geng, 2007: Structures of the northeasternmost South China Sea continental margin and ocean basin: Geophysical constraints and tectonic implications. *Mar. Geophys. Res.*, **28**, 59-79, doi: 10.1007/s11001-007-9014-9. [Link]

Li, C. F., Z. Zhou, H. Hao, H. Chen, J. Wang, B. Chen, and J. Wu, 2008: Late Mesozoic tectonic structure and evolution along the present-day northeastern South China Sea continental margin. *J. Asian Earth Sci.*, **31**, 546-561, doi: 10.1016/j.jseaes.2007.09.004. [Link]

Lin, A. T., A. B. Watts, and S. P. Hesselbo, 2003: Cenozoic stratigraphy and subsidence history of the South China Sea margin in the Taiwan region. *Basin Res.*, **15**, 453-478, doi: 10.1046/j.1365-2117.2003.00215.x. [Link]

Lin, A. T., C. S. Liu, C. C. Lin, P. Schnürle, G. Y. Chen, W. Z. Liao, L. S. Teng, H. J. Chuang, and M. S. Wu, 2008: Tectonic features associated with the overriding of an accretionary wedge on top of a rifted continental margin: An example from Taiwan. *Mar. Geol.*, **255**, 186-203, doi: 10.1016/j.margeo.2008.10.002. [Link]

Liu, H., P. Yan, Y. Liu, and H. Deng, 2006: Existence of Qiongnan suture zone on the north margin of South China Sea. *Chin. Sci. Bull.*, **51**, 107-120, doi: 10.1007/s11434-006-9107-x. [Link]

Liu, Z., 1995: Migration velocity analysis. Ph.D. Thesis, CWP-168, Center for Wave Phenomena, Colorado School of Mines, Golden, USA.

Liu, Z., 1997: An analytical approach to migration velocity analysis. *Geophysics*, **62**, 1238-1249, doi: 10.1190/1.1444225. [Link]

Liu, Z. and N. Bleistein, 1995: Migration velocity analysis: Theory and an iterative algorithm. *Geophysics*, **60**, 142-153, doi: 10.1190/1.1443741. [Link]

Lü, X., P. Yan, J. Chen, H. B. Zheng, and Y. L. Wang, 2009: Application of refraction velocity in studying Mesozoic strata in Chaoshan Depression on northern margin of South China Sea. *J. Trop. Oceanogr.*, **28**, 43-47. (in Chinese)

Shao, L., H. Q. You, H. J. Hao, G. X. Wu, P. J. Qiao, and Y. C. Lei, 2007: Petrology and depositional environments of Mesozoic strata in the Northeastern South China Sea. *Geol. Rev.*, **53**, 164-169. (in Chinese)

Shi, X., H. Xu, X. Qiu, K. Xia, X. Yang, and Y. Li, 2008: Numerical modeling on the relationship between thermal uplift and subsequent rapid subsidence: Discussions on the evolution of the Tainan Basin. *Tectonics*, **27**, TC6003, doi: 10.1029/2007tc002163. [Link]

Sibuet, J. C., S. K. Hsu, X. Le Pichon, J. P. Le Formal, D. Reed, G. Moore, and C. S. Liu, 2002: East Asia plate tectonics since 15 Ma: Constraints from the Taiwan region. *Tectonophysics*, **344**, 103-134, doi: 10.1016/S0040-1951(01)00202-5. [Link]

Taylor, B. and D. E. Hayes, 1980: The tectonic evolution of the South China Sea. In: Hayes, D. E. (Ed.), The Tectonic and Geologic Evolution of South Eastern Asian Seas and Islands, Part 1, AGU Geophys. Monogr., Washington, DC, 23, 89-104.

Taylor, B. and D. E. Hayes, 1983: Origin and history of the South China Sea. In: Hayes D. E. (Ed.), The Tectonic and Geologic Evolution of South Eastern Asian Seas and Islands, Part 2, AGU Geophys. Monogr., Washington, DC, 27, 23-56.

Tillard, S. and J. C. Dubois, 1995: Analysis of GPR data: Wave propagation velocity determination. *J. Appl. Geophys.*, **33**, 77-91, doi: 10.1016/0926-9851(95)90031-4. [Link]

Versteeg, R. J., 1993: Sensitivity of prestack depth migration to the velocity model. *Geophysics*, **58**, 873-882, doi: 10.1190/1.1443471. [Link]

Wang, T. K., M. K. Chen, C. S. Lee, and K. Xia, 2006: Seismic imaging of the transitional crust across the northeastern margin of the South China Sea. *Tectonophysics*, **412**, 237-254, doi: 10.1016/j.tecto.2005.10.039. [Link]

Wessel, P. and W. H. F. Smith, 1998: New, improved version of the generic mapping tools released. *Eos, Trans., AGU*, **79**, 579.

Xia, K. Y., C. L. Huang, and Z. M. Huang, 2004: Upper Triassic-Cretaceous sediment distribution and hydrocarbon potential in South China Sea and its adjacent areas. *China Offshore Oil Gas*, **16**, 73-83. (in Chinese)

Yan, P., H. Deng, and H. Liu, 2006: The geological structure and prospect of gas hydrate over the Dongsha Slope, South China Sea. *Terr. Atmos. Ocean. Sci.*, **17**, 645-658.

Yao, B. C., W. J. Zeng, Y. Z. Chen, X. L. Zhang, D. E. Hayes, J. Diebold, P. Buhl, and S. Spangler, 1994: Xisha Trough of South China Sea - An ancient suture. *Mar. Geol. Quat. Geol.*, **14**, 1-10. (in Chinese)

Yi, H., G. J. Zhong, and J. F. Ma, 2007: Fracture characteristics and basin evolution of the Taixinan Basin in Cenozoic. *Petrol. Geol. Exp.*, **29**, 560-564. (in Chinese)

Yu, H. S. and S. J. Lin, 1991: A preliminary study of seismic stratigraphy of the late Cenozoic Sequences in the Tainan Basin off Southwestern Taiwan. *Terr. Atmos. Ocean. Sci.*, **2**, 75-94.

Zhou, D., 2002: Mesozoic strata and Sedimentary environment in SW Taiwan Basin of NE South China Sea and Peikang High of western Taiwan. *J. Trop. Oceanogr.*, **21**, 50-57. (in Chinese)

Zhou, D., H. Z. Chen, Z. Sun, and H. H. Xu, 2005: Three Mesozoic sea basins in eastern and southern South China Sea and their relation to Tethys and paleo-Pacific domains. *J. Trop. Oceanogr.*, **24**, 16-25. (in Chinese)